# Adsorption of Polyelectrolytes on Chromatographic Columns. Simulated and Experimental Concentration Profiles

**C. Huguenard,† J. Widmaier, A. Elaissari,‡ and E. Pefferkorn***

*Institut Charles Sadron, 6 rue Boussingault, 67083 Strasbourg Cedex, France*

*Received April 8, 1996; Revised Manuscript Received October 16, 1996*[⊗]

ABSTRACT: Using the mobile adsorption model which was previously developed to describe the kinetics of polyelectrolyte adsorption on charged sorbents, we have determined the polyelectrolyte concentration profiles from the amount of polyelectrolyte adsorbed on the successive plates of a chromatographic column resulting from the progressive coverage of the successive plates with species of two different sizes, initially present at equal concentration. This investigation was done with stacked glass microfiber filters (stationary phase) and two fractionated samples of poly(4-vinylpyridine) differing by their molecular weight (flowing phase). Radiolabeling enabled determination of the adsorption of each polyelectrolyte fraction. Selective and fast adsorption of high molecular weight polyelectrolytes detrimental to small polyelectrolytes profoundly modified the concentration profile determined by simulation. This information makes clear some major difficulties inherent in experimental studies of polyelectrolyte adsorption on charged adsorbents.

## Introduction

Solid/neutral polymer solution interfaces have been thoroughly studied from both theoretical and experimental points of view.[1] Equilibrium situations have been considered for monodisperse and polydisperse systems. For the latter systems, relative increased adsorption could be determined for macromolecules of higher molecular weight.[2−6] The kinetics of polymer layer formation has also been investigated, and the rate of initial surface coverage could be described by the random sequential adsorption model.[7]

Hydrosoluble polymers are used in a great number of industrial, agricultural, and environmental applications. Adsorption of these polymers may result from the establishment of hydrogen bonds and/or hydrophobic interactions.[8,9] For polyelectrolytes interacting with charged solids, the phenomena are more complex and the previous forces were found to exert a role concomitantly with charge−charge interactions in a great number of polyelectrolyte−sorbent systems.[10,11] A strong polymer−solid interaction is usually required in purification processes where a nonselective flocculation should operate. However, for the selective flocculation of mineral oxides,[12] polyelectrolytes developing low energy interactions may be potentially more effective. In the presented study our aim was to investigate the interfacial behavior of such polyelectrolytes. Since hydrogen bond formation and hydrophobic interactions may lead to irreversible adsorption,[13] it was essential to choose an experimental system in which only electrostatic forces were responsible for adsorption. This situation corresponds to "true" polyelectrolytes whose solution behavior is dictated only by electrostatic interactions between charged chain elements and adsorption behavior at charged solid−liquid interfaces caused by polyion−surface charge interactions. The adsorption/desorption processes at equilibrium are induced by variations of the polymer free energy.

Poly(4-vinylpyridine) (PVP) at pH 3 was found to display such solution and interfacial characteristics.[14] Reversibility of adsorption does not mean that the adsorbed polymer immediately desorbs when the supernatant solution is replaced by solvent, and desorption of adsorbed PVP was found to be a very slow process developing over hours. The initial fast coverage could be schematically represented by the mobile adsorption process which combines random sequential adsorption and in-plane diffusion.[7] Random sequential adsorption implies that the species sequentially attempt to adsorb on a plane, the contact point being chosen randomly. Adsorption succeeds at the selected position when the surface area is free of adsorbed species and fails when the chosen area is already occupied.[15,16] The in-plane diffusion model modifies the first model by allowing the adsorbed macromolecule to move freely on the adsorbent surface. This model adequately described the adsorption kinetics and provided an interpretation for the adsorption reversibility of PVP.[7]

Numerous studies have addressed adsorption of polyelectrolytes characterized by a small polydispersity in molecular weight and have voluntarily excluded or ignored selective adsorption resulting from the use of polydisperse samples.[17,18] Selective adsorption from a mixture of pure polyelectrolytes differing only by their molecular weight has not been studied before and is the aim of the present investigation.

In a previous paper we presented results on chromatographic separation induced by surface exclusion chromatography.[19] A diblock copolymer solution containing isolated molecules and micellar assemblies was injected into a chromatographic column composed of stacked glass microfiber filters. This technique provided information on the composition of the injected solution by comparing the experimental concentration patterns inside the column and those simulated by application of the random sequential adsorption (localized adsorption) model to the successive plates of the column.[20] In this paper we present the adsorption situation resulting from injection of an equimolar mixture of two PVP samples of different molecular weight. As previously, the adsorption of each polyelectrolyte sample was determined as a function of the filter position. The present experiment was simulated using the algorithm

* Author to whom correspondence should be addressed.
† Present address: UMR 50, RMN et Chimie du Solide, Institut Le Bel, 4 rue Blaise Pascal, 67070 Strasbourg Cedex, France.
‡ Present address: Unité Mixte CNRS-BIOMERIEUX, Ecole Normale Supérieure de Lyon, 46 Allée d'Italie, 69364 Lyon Cedex, France.
⊗ Abstract published in *Advance ACS Abstracts,* February 15, 1997.

S0024-9297(96)00515-3 CCC: $14.00 

**Table 1. Solution and Interfacial Characteristics**

| code | $M_w$ (g/mol) | $N$ | $R_G$ (nm) | Spec act. $\times 10^9$ (cpm/g) | $N_S^* \times 10^{11}$ (mol/dm$^2$) | $N_S^* \times M_W$ ($\mu$g/dm$^2$) | $N_S \times 10^{11}$ (mol/dm$^2$) |
|---|---|---|---|---|---|---|---|
| f2 | 1 057 000 | 10 067 | 61.3 ± 0.5 | 1.83 | 0.14[a] − 0.12[b] | 1.5[a] − 1.4[b] | 0.14[c] − 0.17[d] |
| f6 | 78 500 | 748 | 18.5 ± 1.5 | 1.75 | 1.32[b] | 1.0[b] | 1.3[c] − 1.65[d] |

[a] From the RSA model. [b] From eq 3. [c] From Figure 9b. [d] From Figure 9c.

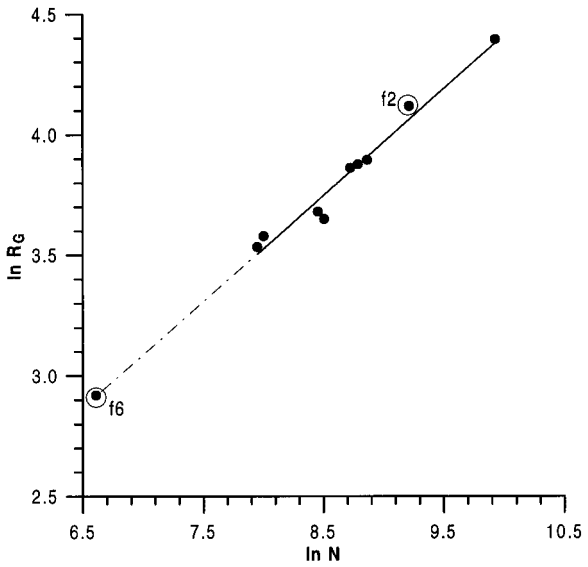


**Figure 1.** PVP in 0.01 M NaCl ethanolic solution. Representation of the radius of gyration ($R_G$, nm) as a function of the polymerization index ($N$) determined from light scattering measurements. The circled symbols correspond to the fractionated samples employed in chromatographic experiments.

of the mobile adsorption process and the corresponding concentration profile was compared to the experimental pattern.[20]

Adsorption of PVP was found to present interesting interfacial characteristics. The adsorbed chain undergoes reconformation in the adsorbed state,[21] which could be highlighted by controlling the rate of polymer supply to the adsorbent.[14,22] Reconformation was found to control the rate and mechanism of the destabilization of colloid−polymer complexes.[23] On the other hand, when the molecules are supplied to the surface at a fast rate, reconformation should induce an overlap of adsorbed coils, which is impeded by a rapid eviction of the molecules being adsorbed in excess.[14] The interfacial structure is independent of the rate of polymer supply since low reconformation during adsorption or rapid desorption of chains being adsorbed in excess led to a unique equilibrium structure of the adsorbed chain. Therefore, to establish the equilibrium situation, fast elution conditions were imposed during chromatography, and the expected effect of the rapid desorption process was taken into account in designing the chromatography.

## Experimental Section

**1. Materials.** PVP was synthesized in ethylene glycol using azobisisobutyronitrile as initiator. After purification by successive precipitations in alkaline water and dissolution in ethanol, the polymer was fractionated in methanol−toluene mixtures. The polymerization index ($N$) and the radius of gyration ($R_G$) of the different samples were determined from light scattering measurements in 0.01 M NaCl ethanolic solution to obtain information on the geometrical dimensions. Figure 1 shows the correlation existing between $R_G$ and $N$, which is expressed as follows:

$$R_G\,(\text{nm}) = 0.94N^{0.45} \quad (1)$$

The value 0.45 of the exponent, slightly smaller than the theoretical value of 0.5 expected in Θ solvent, may result from polydispersity effects. Due to the various polymer species inevitably present even in a well-fractionated polymer, one expects the theoretical correlation to apply to $R_G$ and $M_Z$ while in eq 1 0.45 correlates $R_G$ with $N$, which was calculated using $M_w$, $M_Z$ and $M_w$ being the $Z$- and weight average molecular weights, respectively.

It is well-known that the efficiency in precipitation fractionation increases as the molecular weight decreases and that every fraction contains an appreciable amount of the lower molecular components (the tail effect), an inherent characteristic of fractional precipitation. More precisely, the transfer of polymer of higher polymerization index from the dilute medium to a concentrate one is accompanied by a parasitic transfer of polymer of very small molecular weight due to the initially high polymer concentration.[24] Therefore, the first fraction (f1) was discarded to limit such effects. The two samples indicated by surrounded symbols were employed in the adsorption experiments for reasons developed in 3. Simulation of Chromatography and also because the molecular weights were estimated to be sufficiently different (3 orders of magnitude) so that the molecular weight of the smallest polymer in f2 should be greater than that of the largest one in f6.

In order to determine precisely the polymer concentrations in very dilute solution and the amounts of polymer adsorbed on the glass microfiber filters, radiolabeled PVP samples of the two fractions were obtained by quaternization with $I^{14}CH_3$ of a few pyridine groups (0.1%) in ethylene glycol solution. The molecular characteristics and specific radioactivity of the samples f2 and f6 are given in Table 1.

**2. Chromatographic Column.** The chromatographic column is composed of a calibrated glass syringe (Tacussel, Lyon, France) and the corresponding pistons, which were modified to be fitted with input and output apertures of 0.5 mm, allowing the polymer solution to be injected at one point at a controlled rate with the aid of an automatically driven syringe and recovered at the other one. Two 2 mm thick "nonadsorbing" Teflon disks of large porosity were clamped close to the input piston inside the column to establish a homogeneous distribution of the injected solution through the successive Whatman glass microfiber filters GF/B whose retention is limited to particles above 1 $\mu$m.[25] Each filter had a diameter of 5 mm and a thickness of 1.4 mm, the calculated mean diameter of the glass microfiber being close to 6 $\mu$m. The amount of polyelectrolyte adsorbed on these two nonadsorbing Teflon disks is reported in Figures 6−10 to indicate the absence of polyelectrolytes retention and/or fractionation by adsorption. The column was filled with 56 filters and the height of the adsorbent in the column was reduced from 8 to 4.5 cm after stacking. The silica volume thus represented 10% of the void volume of the column, which was equal to 0.77 mL. The column was then initially carefully saturated and eluted with acidic water at pH 3.0 to establish reproducible adsorption characteristics on the solid−liquid interface.

Our assumption of identical specific adsorption of PVP on glass microfibers and polystyrene latex particles which have been employed in previous works is based on the following experimental results. In batch experiments the adsorption on the two adsorbents was found to be reversible when the supernatant polymer solution was progressively replaced by pure solvent. This excludes all adsorption mechanisms such as hydrogen bonding or hydrophobic interaction but militates in favor of charge−charge interactions. Moreover, at the pH of the experiments, silica and polystyrene latex particles are

characterized by a surface charge density on the order of 2.8 $\mu$C/cm$^2$. From adsorption measurements of PVP of molecular weight $3.6 \times 10^5$ on polystyrene latex particles, the surface area available to polymer adsorption was estimated to be 1 dm$^2$/filter.

**3. Chromatography.** The polymer solution was injected at a controlled rate. The sustained flow of polymer solution moved down the column, enabling the polymer to be adsorbed onto the successive filters. When the fixed volume of solution was injected through the column, the injection was stopped. Elution is continued with solvent, or in some instances, the solution in the void volume is pushed out. The filters were successively taken out of the column with care, individually deposited into glass vials containing scintillation liquid, and counted for radioactivity content using a Tricarb spectrometer (Packard). The radioactivity (cpm) of each filter was converted to the number of adsorbed polyelectrolyte, and the chromatogram was obtained by plotting the adsorbed amount (mol/dm$^2$ or $\mu$g/dm$^2$) as a function of the filter number. For elution with a mixture of two polymers of different molecular weight, only one of the two polymer samples was radiolabeled and the experiment duplicated to determine the adsorption amounting to each polyelectrolyte. The parameters used in the experiments are the polyelectrolyte concentration in solution ($C_0$) (mol/mL), the injection rate ($J_V$) (mL/min), and the rate of polyelectrolyte supply ($J_V C_0$) (mol/min).

## Situation of the Numerical Adsorption Model

**1. Monodisperse Polyelectrolytes at Interfaces. A. Empirical Model.** We previously determined that the number of macromolecules forming a polymeric monolayer ($N_S$*) may be empirically estimated on the same basis that can be used for the calculation of the critical concentration ($c$*) of nonoverlapping spheres in three dimensions:[14]

$$c^* = \frac{0.77}{[\eta]} = \frac{0.77^* M_w}{\Phi R_G{}^3} \qquad (2)$$

$$N_S{}^* = \frac{0.84}{([\eta]M_w)^{2/3}\, N_A{}^{1/3}} = \frac{0.84}{\Phi^{2/3} N_A{}^{1/3} R_G{}^2} \qquad (3)$$

$\Phi$ being equal to $3.3 \times 10^{24}$ (cgs) and $N_A$ being Avogadro's number. It is important to note that the intrinsic viscosity or radius of gyration of polyelectrolyte should be determined from measurements in an appropriate solvent. Application of eqs 2 and 3 to poly(4-vinylpyridine) of molecular weight equal to $3.6 \times 10^5$ led to values of $N_S$* equal to $1.8 \times 10^{-12}$ and $7 \times 10^{-12}$ mol/dm$^2$ when the molecular characteristics were determined in water and ethanol, respectively. The experimental value was found to be $8.3 \pm 0.3 \times 10^{-12}$ mol/dm$^2$, and the correspondence between the experimental value and that determined in ethanol calls for the following comment. It is well-known that the reduced viscosity of polyelectrolytes strongly increases with dilution as a result of the effect of increasing electrostatic repulsive forces. These forces are screened when the polyelectrolytes are solubilized in concentrated or electrolytic solutions or adsorbed at solid−liquid interfaces. To obtain molecular characteristics of polyelectrolyte exclusive of electrical charge effects, the intrinsic viscosity and radius of gyration were determined in ethanol. The critical characteristics of adsorption may be calculated from eqs 2 and 3, and the number of moles and mass adsorbed are reported in Table 1.

**B. Maximal Coverage in Random Sequential Adsorption.** The previous monolayer model may be improved if one consider that the kinetics of adsorption may be described by the random sequential adsorption model combined to in-plane diffusion. The previous assumption of screening of long range interactions in the solid−liquid interface permits us to calculate the surface coverage using the simple model of disk adsorption which ignores electrical charge interactions.[26,27] Therefore, the radius of gyration was determined in concentrated electrolyte media to appraise the interfacial area of the adsorbed molecule being excluded for further adsorption. Figure 2 represents the intrinsic viscosity (cgs) of the fractionated sample f2 as a function of pH in 0.05, 0.1, and 0.5 M NaCl solutions. Since the decrease in ionic strength and protonation of pyridine groups induce a swelling of the polyelectrolyte coil, we assumed that unperturbed dimensions correspond to $[\eta]$ determined in 0.5 M NaCl. Taking into account this value of $[\eta]$, the corresponding value of $R_G$ (eq 2), and the relative surface area of 0.54 available for adsorption of disks in the random sequential adsorption,[26] we calculated the amount of f2 which can be adsorbed to be 1.5 $\mu$g/dm$^2$. Since the polyelectrolyte comes from a dilute aqueous solution, we first assume that the polyelectrolyte maintains its solution conformation in electrolyte free medium when it collides with the adsorbent surface. Secondly, the adsorption area which is thus excluded should be proportional to the radius of gyration (or intrinsic viscosity) determined in the absence of all charge−charge interactions ($R_m$). This scheme clearly describes the situation of noninteracting adsorbed disks. However, when we take into account that polymer tails are protruding toward the salt free aqueous solution, interactions between protonated pyridinium groups are expected to induce long range repulsive forces between occupied areas and adsorbing polyelectrolytes while interactions between negatively charged polymer free areas and adsorbing polyelectrolytes are expected to induce attractive forces. This scheme is in agreement with our random sequential adsorption model combined with in-plane diffusion (mobile adsorption).

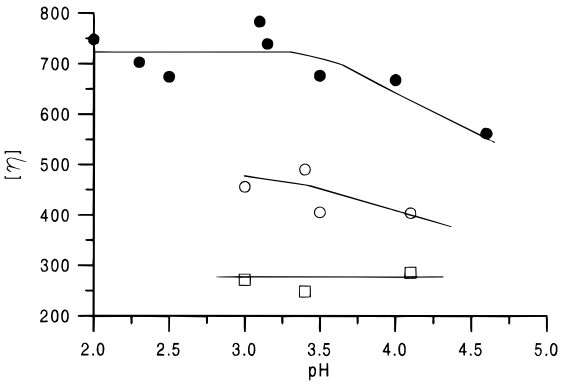


**Figure 2.** PVP in aqueous NaCl solution. Representation of the intrinsic viscosity $[\eta]$ (mL/g) as a function of pH for different ionic strengths of the solution: (●), 0.05; (○), 0.1 and (□), 0.5.

**C. Reconformation on Saturated Interfaces.** The experiments which evidenced the reconformation of adsorbed chains have been reported elsewhere.[14] This phenomenon can be briefly described as follows: when the molecules are rapidly supplied to the adsorbent, the surface area is filled with macromolecules characterized by an interfacial area corresponding to solution characteristics (acidic water at pH 3.0) and an exclusion area proportional to $R_m$. This does not correspond to an equilibrium situation, and since the adsorbed polyelectrolytes are strongly constricted in the layer, approximately one-half of the macromolecules apparently being

in excess become rapidly ejected from the surface. The kinetics of the process could be interpreted by assuming an increase in the radius of the exclusion area of the adsorbed polyelectrolyte ($R$) such as

$$\frac{R_2 - R_{ads}^2}{R_m^2 - R_{ads}^2} = \exp\left[-\frac{t}{\tau_{des}}\right] \quad (4)$$

where the indices m and ads refer to initial and equilibrium situations at full coverage, respectively. The relaxation time ($\tau_{des}$) was found to be on the order of 10 min for a polyelectrolyte of molecular weight equal to $3.6 \times 10^5$. Nothing at present is known about the possible dependence of $\tau_{des}$ with molecular weight.

Interfacial reconformation should result here from the strong interaction existing between the positively charged pyridinium groups of the polyelectrolyte and the negatively charged groups on the silica surface. Moreover, it is expected that the close vicinity of these two groups would induce an enhanced charge−charge interaction which has been determined for aqueous solutions of the symmetrical diblock copolymer poly(styrene sulfonate)−poly(vinylpyridine).[28]

**2. Mechanism and Kinetics of Surface Coverage.** The first mechanism corresponding to the initial step of polymer deposition on bare surfaces resembles a random sequential adsorption (RSA) process if the adsorption is irreversible.[7] This RSA has been modified in order to take into account the situation of polyelectrolytes in aqueous medium. First, polyelectrolyte adsorption resembles ion-exchange and as a result, since the polyelectrolyte position in the adsorption plane is not definitely fixed, the polymer remains able to move freely in the adsorption plane. Secondly, long range forces may give an adsorbing macromolecule a greater possibility of finding a free area by deviating from the initial trajectory when a molecule is already adsorbed at the target.[20] Third, internal mobility implies adsorption reversibility when certain parameters of the supernatant, such as the polymer concentration and/or molecular weight, are modified. In our numerical study, only the two first points have been directly considered and the third point will be discussed when the simulation and experimental results are compared.

The random sequential adsorption algorithm was therefore adapted to take into account that an adsorbing disk is attracted by free portions and repelled by covered areas of the adsorbent surface. When a randomly selected position is already occupied, adsorption does not immediately fail but the disk will search for a free area in the close vicinity. However, as the term "close vicinity" indicates that disk−disk or disk−sorbent interactions cannot greatly modify the position of adsorption relative to the initial randomly fixed coordinates, the maximum length of the walk is an important parameter. Adsorption occurs if the disk finds a free area, but if no free area is encountered during the random walk, the adsorption attempt definitively fails. In order to determine the characteristics of the random walk, we consider the following two situations: a disk of radius $r_1$ encounters an area occupied by a disk of radius $r_2$, or a disk of radius $r_2$ encounters an area occupied by a disk of radius $r_1$. The unidirectional diffusion path allowing both disks to escape from the occupied position is given by

$$(r_1 + r_2)^2 = 2(\nu/6)L^2 \quad (5)$$

where $L$ is the length of the elementary jump, and $\nu$ is the maximal number of jumps. Since only interfacial characteristics are taken into account, an adsorbed disk of large radius $r_2$ is considered to more effectively screen the attractive interaction between an adsorbing disk of $r_1$ and the plane than an adsorbed disk of $r_1$ for an adsorbing disk of $r_2$. This condition is fulfilled by correlating the jump length ($L$) with the radius of the disk attempting to adsorb ($r_a$):

$$L \approx r_a^f/\lambda \quad (6)$$

Large values of $\lambda$ ensure the best positioning of an adsorbing disk when the available area is located between a set of adsorbed disks or is close or equal to the area of the disk attempting to adsorb. Positive values of $f$ are essential in the model. The corresponding physically unrealistic assumption of an increase of the diffusive mobility of disks of radius $r_2$ is equivalent to the more realistic assumption of a decrease in the in-plane mobility of that disk. Therefore, a large adsorbed disk moves too slowly in the adsorption plane to facilitate by its own displacement the adsorption of small disks. Similarly, an increased mobility of large disks in solution implies an increased mobility of the small disks in the adsorbed state. A small adsorbed disk is able to move rapidly in the plane and hence more readily allows successful adsorption of large disks. The exponent $f$ in eq 6 thus scales the energy of the disk−plane interactions: $f = 1$ corresponds to the in-plane mobility of the adsorbed disk being inversely proportional to the square root of its area, while $f = 2$ indicates that the mobility is proportional to its area. From a physical point of view, $f = 1$ may describe the interfacial characteristics of loose solutes like synthetic macromolecules ($f = 1$ was chosen for the present situation) whereas $f = 2$ may apply to more dense species like proteins.

The second parameter was the jump frequency ($\nu$), and its influence on the selectivity of disk adsorption has been determined previously.[20] At the level of each plate, each disk was allowed to undergo a random walk in two dimensions limited to 500 jumps, the lengths of each jump being 0.1 and 0.3 for disks of radius 3 and 1, respectively.

**3. Simulation of Chromatography.** In simulation, the chromatographic column is schematized by successive adsorbing square plates and, obviously, the real chromatographic system cannot be exactly simulated. Since the coordinates of each jump had to be tested for success or failure in adsorption, the set of the simulation parameters (number of disks and plates, plate area) was critically determined to mimic the experimental chromatography. To also save computer time, we employed the following model: (i) 250 disks of radius 1 and 250 disks of radius 3 are mixed in a box and (ii) the disks to be successively injected in the column were randomly chosen among these 500 disks. This procedure was repeated 250 times. The plate area was limited to 62 500 in order to obtain a surface coverage across about 60 plates. Disks failing to adsorb on plate $i$ attempt to adsorb on plate $(i + 1)$ and so on. In this simulation, there is no possibility for selective adsorption by replacement of small disks by large ones or the converse. For each plate $i$, we determined the total number of adsorbed disks, the number of adsorbed disks of radii 1 and 3, and the fractional covered area. Experimental results using polyelectrolytes f2 and f6 (the radii of

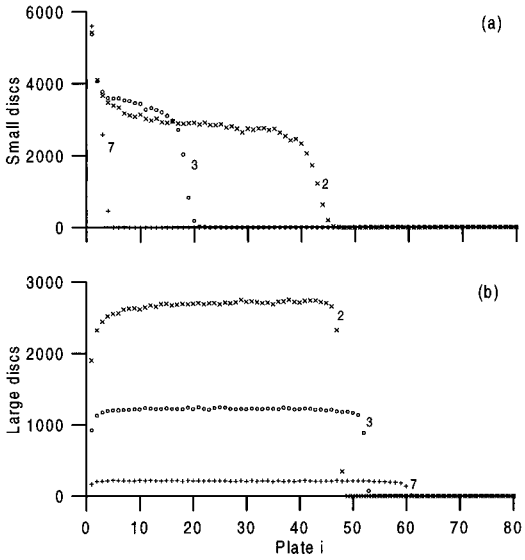


**Figure 3.** Representation of the number of small (radius = 1) (a) and large (radius = 2, 3 and 7) (b) disks adsorbed as a function of plate number (i) for the mobile adsorption model. The radius of the large disk is indicated on the curve, and the initial relative concentration of the two types of disks is 0.5.

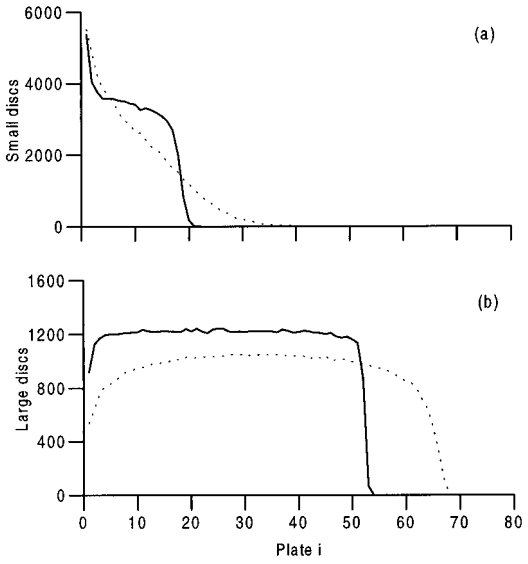


**Figure 4.** Representation of the number of small (radius = 1) (a) and large (radius = 3) (b) disks adsorbed as a function of plate number (i) for mobile (full line) and localized (dashed line) adsorption models. The initial relative concentration of the two types of disks is 0.5.

gyration being in the ratio 1/3.3) and numerical results may be compared as far as we are interested in the relative distribution of small and large disks onto successive filters and plates. The simulation study was extended to two different systems (disks of radii 1 and 2 or 1 and 3) in order to determine the corresponding evolution of the chromatograms. The different simulations combining runs of 500 (disks of radii 1 and 2), 250 (disks of radii 1 and 3), and 50 injections (disks of radii 1 and 7) led to the same total surface area coverage.

## Results

**1. Simulation.** Parts a and b of Figure 3 show the number of small (a) and large disks (b) adsorbed as a function of plate number *i* for different values of the radius of the large disk: 2, 3, and 7. For the mixture of disks of radii 1 and 7, the small disks are adsorbed on the four initial plates. For the mixture of disks of radii 1 and 3, the small disks are distributed over the first 17 plates whereas the end of the column is only covered with large disks. In the plateau region the number of small disks is about 3 times greater than that of the large ones. For the mixture of disks of radii 1 and 2, Figure 3 shows that an equal number of small and large disks is adsorbed throughout the column and that only the end of the column is covered with disks of unique size.

Experiments using polyelectrolytes characterized by radii of gyration being in a ratio 1/7 are unworkable with fractions being at hand. On the other hand, the simulation with disks of radii 1 and 2 shows that, apart from the first five plates, there is no real separation between the two species. Obviously, the system combining disks of radii 1 and 3 presents a major interest as far as the simulation induces a detectable overadsorption of small disks on the first third of the column and an adsorption of large disks exclusive of small ones on the second portion. Figures 4 and 5 represent the detailed results of this simulation. Figure 4 shows the number of small (a) and large (b) disks/plate as a function of the plate number *i*. Figure 5 shows the total number of adsorbed disks (a) and the covered area (b). The straight lines correspond to the present simulation

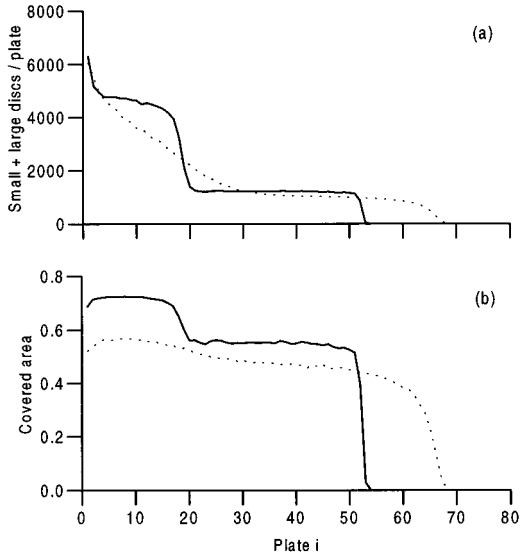


**Figure 5.** Representation of the total number of adsorbed disks of radii 1 and 3 (a) and relative total coverage by adsorbed disks (b) as a function of the plate number (i) for mobile (full line) and localized (dashed line) adsorption models. The initial relative concentration of the two types of disks is 0.5.

and the dashed lines correspond to the pure RSA model, which prevents in-plane mobility. The mobile process allows an increased adsorption of the large disks throughout the column if compared to the RSA situation. For the small disks, the situation is more complex: for plates 1−5, the RSA allows more disks to adsorb whereas the inverse situation is observed for plates 5−16. The mobile adsorption model allows the surface covering to be more complete in the initial zone of the column where small disks are adsorbed preferentially, as illustrated in Figure 5a,b. In the zone of maximal covered area (the first plates being excluded as shown in Figure 5b, the relative occupied areas are 0.544 and 0.180 for disks of radius 3 and 1, respectively, and the number of small disks is 3-fold that of large disks. Obviously, since an excess of small adsorbed disks is expected to exclude the centers of large disks

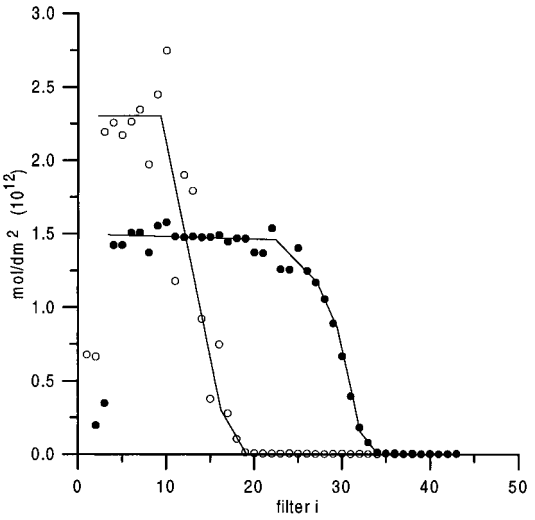


**Figure 6.** Experimental chromatogram for elution with fractionated sample f2. Representation of the number of moles adsorbed per filter (area = 1 dm$^2$) as a function of the filter number (i). Open symbols correspond to the following parameters: $C_0 = 1.01 \times 10^{-10}$ mol/mL, $J_V = 0.15$ mL/min, $t = 2$ min, and $J_V C_0 = 1.51 \times 10^{-11}$ mol/min. Filled symbols correspond to $C_0 = 1.05 \times 10^{-11}$ mol/mL, $J_V = 1.5$ mL/min, $t = 2.5$ min and $J_V C_0 = 1.58 \times 10^{-11}$ mol/min.

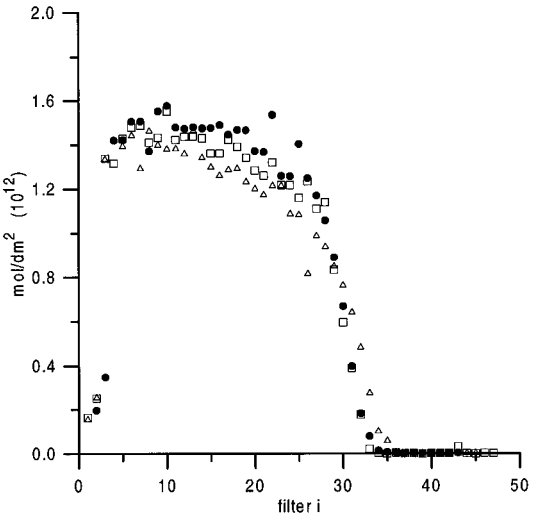


**Figure 7.** Experimental chromatogram for elution with fractionated sample f2. Representation of the number of moles adsorbed per filter (area = 1 dm$^2$) as a function of the filter number (i). The parameters are as follows: $C_0 = 1.05 \times 10^{-11}$ mol/mL, $J_V = 1.5$ mL/min, $t = 2.5$ min, and $J_V C_0 = 1.58 \times 10^{-11}$ mol/min. No solvent injection (●) and 5 mL (□) and 10 mL solvent injection (△).

and strongly reduce the covered area in the first plates, the resulting modification of the elutant composition progressively leads to an optimal elutant composition which is strictly suited to allow such optimal coverage: the relative surface area occupied by large disks is equal to that which is covered when only large disks are injected and is close to the jamming limit of 0.547.

**2. Experiments.** We present first chromatograms obtained for injection of solutions only containing one fraction.

**A. Effects of Polyelectrolyte Concentration and Injection Rate.** The rate of supply ($J_V C_0$) of the fraction f2 was kept constant and equal to $1.5 \times 10^{-11}$ mol/min, whereas $C_0$ was $1.05 \times 10^{-11}$ and $1.01 \times 10^{-10}$ mol/mL for $J_V = 1.5$ and 0.15 mL/min, respectively. Figure 6 shows the amount of polyelectrolyte adsorbed on the successive filters (mol/dm$^2$), each filter developing a surface area equal to 1 dm$^2$. A fast injection rate of a dilute solution limits the period for which polymers statistically face a given filter, while a low injection rate of a concentrated solution increases the adsorption probability. Therefore $C_0$ and $J_V$ are not interchangeable when only a limited amount is injected into the column.

**B. Effect of Reconformation at Saturation.** The sample f2 at a concentration of $1.05 \times 10^{-11}$ mol/mL was injected for 2.5 min at 1.5 mL/min. The experiment was repeated twice with solvent injection for 6 and 9 min after polymer injection. Although the polymer in the void (the balance between injected and adsorbed polymer being less than $1.4 \times 10^{-13}$ mol) was negligible in comparison to the polymer adsorbed, the interstitial solution was replaced by solvent at the end of each elution. Figure 7 shows that the concentration shape does not strongly depend on the rinsing period.

A second set of experiments with a more concentrated solution ($1.01 \times 10^{-10}$ mol/mL) injected for 14 min at 0.15 mL/min provided the results reported in Figure 8. This experiment was also repeated twice, the solvent being injected for 5 and 10 min after polymer injection. Aging of the interfacial layer induces a decrease of the surface coverage, which may be attributed to a slight

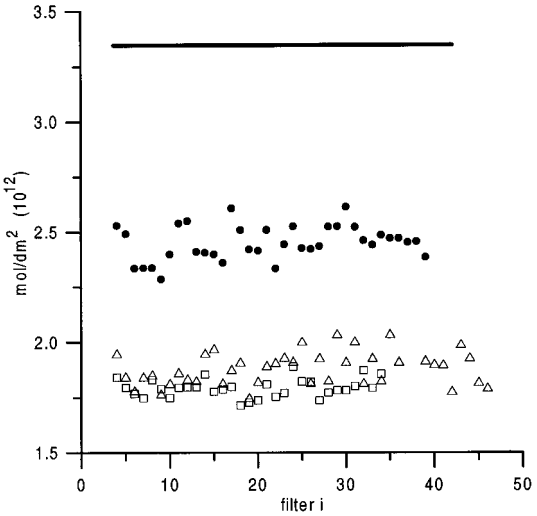


**Figure 8.** Experimental chromatogram for elution with fractionated sample f2. Representation of the number of moles adsorbed per filter (area = 1 dm$^2$) as a function of the filter number (i). The parameters are as follows: $C_0 = 1.01 \times 10^{-10}$ mol/mL, $J_V = 0.15$ mL/min, $t = 13.5$ min, and $J_V C_0 = 1.51 \times 10^{-11}$ mol/min. No solvent injection (●) and 10 mL (△) and 15 mL (□) solvent injection. The straight line gives the theoretical surface coverage prior to polyelectrolyte relaxation.

collapse of the adsorbed polymer. The straight line indicates the coverage at the theoretical time zero (no relaxation) to be close to $3.3 \times 10^{-12}$ mol/dm$^2$. The final piece of quantitative information is that the interfacial area occupied by one adsorbed macromolecule is doubled under these adsorption conditions as previously observed.[14]

**C. Excluded Area for Fractions f2 and f6.** Figure 9a,b shows the adsorption chromatograms obtained for injection at 1.5 mL/min of pure samples f2 and f6 at equal concentrations of $1.05 \times 10^{-11}$ mol/mL during 2.5 min for f2 and 14 min for f6. Figure 9a presents the amount of polymer adsorbed expressed in $\mu$g/dm$^2$ and Figure 9b shows the same information in mol/dm$^2$. After injection of the pure sample f2 (0.15 mL/min for 14.5 min) and f6 (1.5 mL/min for 5 min) at $1.05 \times 10^{-10}$ mol/mL and rapid washing of the column with solvent,

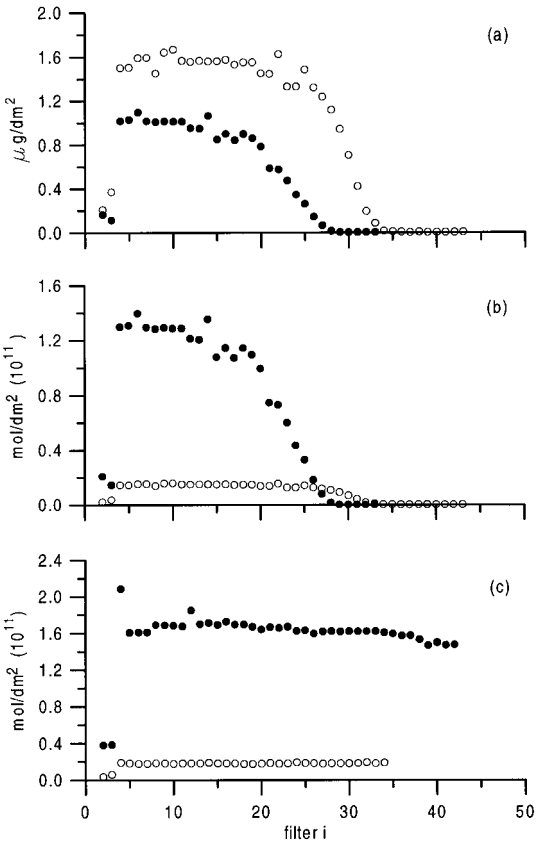


**Figure 9.** Experimental chromatograms for elution with fractionated sample f2 (○) and f6 (●). Representation of the number of micrograms (a) and moles (b) adsorbed per filter (area = 1 dm$^2$) as a function of the filter number (i). The parameters of the elution with f2 are $C_0 = 1.05 \times 10^{-11}$ mol/mL, $J_V = 1.5$ mL/min, $t = 2.5$ min, and $J_V C_0 = 1.58 \times 10^{-11}$ mol/min and with f6 are $C_0 = 1.0 \times 10^{-11}$ mol/mL, $J_V = 1.5$ mL/min, $t = 14$ min, and $J_V C_0 = 1.50 \times 10^{-11}$ mol/min. (c) The number of moles adsorbed per filter (area = 1 dm$^2$) as a function of the filter number (i). The parameters of the elution with f2 are $C_0 = 1.01 \times 10^{-10}$ mol/mL, $J_V = 0.15$ mL/min, $t =$ 14.5 min, and $J_V C_0 = 1.51 \times 10^{-11}$ mol/min and with f6 are $C_0 = 1.48 \times 10^{-10}$ mol/mL, $J_V = 1.5$ mL/min, $t = 5$ min, and $J_V C_0 = 2.22 \times 10^{-10}$ mol/min.

we obtain the chromatogram represented in Figure 9c. Comparison between the theoretical $N_S$* and experimental $N_S$ values of the adsorption amount (Table 1) led us to conclude that (i) the full area of the glass microfiber filter is available to adsorption for both fraction f2 and f6 and (ii) the polyelectrolyte f2 effectively occupies an interfacial area 9-fold larger than fraction f6, which could be validly compared to a value of 13.3, which was calculated from the radii of gyration. The difference in the adsorption amounts of 1 and 1.6 $\mu$g/dm$^2$ may result from the variation of the density of polymer chain segments already existing in solution.[28,29] Finally, the adsorption of f2 experimentally determined is comparable to the value calculated using the RSA model (see Table 1).

**D. Chromatograms Obtained from Equimolar Mixtures of f2 and f6.** This experiment was duplicated, and equimolar mixtures contained at once a radiolabeled sample of one polyelectrolyte and a nonlabeled sample of the other. Injecting mixtures at a total concentration of $2 \times 10^{-10}$ mol/mL at 0.15 mL/min for 15 min and rapid washing with solvent provide the histograms of Figure 10. The solid line represents the previous situation of injection of f2. The amount of polymer injected into the column corresponded to a full

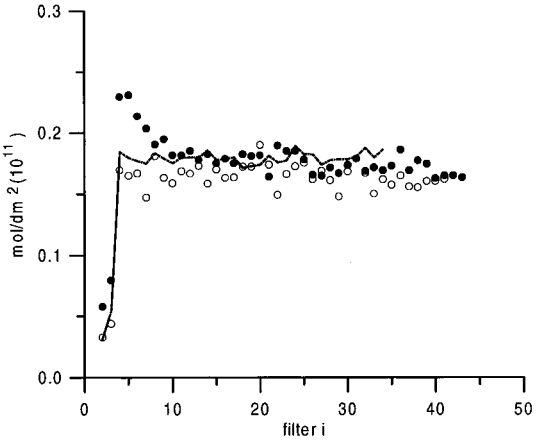


**Figure 10.** Experimental chromatograms for elution with an equimolar mixture of fractionated samples f2 (○) and f6 (●). Representation of the number of moles adsorbed per filter (area = 1 dm$^2$) as a function of the filter number (i). The parameters of the elution for each sample are $C_0 = 1.05 \times 10^{-10}$ mol/mL, $J_V = 0.15$ mL/min, $t = 15$ min, and $J_V C_0 = 1.5 \times 10^{-11}$ mol/min. The line represents the situation of injection of the pure f2 given in Figure 9c.

coverage of about 130 filters. This number should be compared to the 54 plates covered in simulation by small and large disks (Figures 5a,b). Since Figure 4a reveals coadsorption of small and large disks on 17 plates, we investigated the type of coverage on the equivalent 40 microfiber filters, where simulation predicted coadsorption of fractions f6 and f2.

The results of Figure 10 may be interpreted on the basis of the mobile adsorption model since adsorption of $0.17 \times 10^{-11}$ mol/dm$^2$ effectively corresponds to the jamming limit, which cannot be outnumbered. On the first filters, a slightly denser occupation by the polyelectrolyte f6 can be noted, as expected from Figure 4a. The plateaus indicate equal adsorption of polyelectrolytes f2 and f6 whereas, according to our simulation, the number of moles of f6 was expected to be 3-fold greater than that of f2. This implied that the solution continuously flowing through the column is more enriched in f6 than determined from simulation and, on the average, is always identical to the mixture being injected into plate 1. Therefore, the surface coverage and the number of large disks being adsorbed on plate 1 for injection of an equimolar mixture should be recovered on the successive plates because the injected mixture remained equimolar on average. Figure 3b shows that the number of disks of radius 3 on plate 1 is only equal to 75% of the number corresponding to the jamming limit (plateau value), so we expect that the maximal coverage by polyelectrolytes f2 should not exceed $0.75 \times 0.17 \times 10^{-11}$, that is, $0.13 \times 10^{-11}$ mol/dm$^2$.

The unexpected adsorption of $0.17 \times 10^{-11}$ mol/dm$^2$, determined experimentally may be interpreted as follows. Our schema reveals a situation of selective adsorption of large disks when the total area allotted to a set of adjoining small disks is large enough to allow adsorption of one large disk. Therefore, at any moment, one large disk replaces the corresponding set of small disks which again attempt to adsorb on the subsequent plates. Therefore, for selective reversible adsorption, the situation will be similar on each plate and the histogram of the size exclusion chromatography will be flat. Similarly, one polyelectrolyte f2 may replace several adsorbed polyelectrolytes f6 when the positions of f6 are distributed in such a way that the areas

belonging to f6 and the interstitial areas are large enough. Conversely, when the area portions are too small to allow mobile adsorption of f2, the interfacial exchange is impeded.

## Summary

A major contribution of the chromatographic study is an improvement of our representation of an adsorbed polyelectrolyte. The area excluded by adsorption of the mobile type can be determined from its conformation in electrolyte solution of high ionic strength, where long range forces are screened. However, this representation does not mean that the adsorbed polyelectrolyte chain is only confined in this area, and we infer that the disk-like exclusion area corresponds to the central polymer zone of dense interfacial occupation by chain segments, whereas the large outer zone of smaller density does not exclude adsorbing molecules and enables penetration of identical zones by adsorbed neighbors. Our assumption that an adsorbing polyelectrolyte is expected to be deviated from its initial trajectory by a chain already adsorbed is based on the existence of a zone of smaller density (loops and tails of adsorbed polyelectrolyte, outer chain segments of the polyelectrolyte in solution) bearing charged groups with the effect of increasing the range of electrical forces between adsorbed and adsorbing flat disks. Thus, the image of polyelectrolytes at a solid−water interface may reveal well interconnected chains for which the positions are nevertheless fixed by the mobile adsorption model.

Despite the fact that surface and initial solution compositions are similar in our experiments, comparisons between experimental and numerical chromatograms clearly demonstrates that the adsorption selectivity greatly favors surface coverage with polyelectrolytes of high molecular weight. The exchange between polyelectrolytes of small and high molecular weights is relatively fast in comparison to the slow relaxation previously observed during delayed adsorption but is comparable to the expulsion/desorption phenomenon which was observed at surface saturation.[14] Since the final area covered with polyelectrolytes of large molecular weight corresponds to the maximal coverage, small polyelectrolytes occupying the remaining surface area cannot exchange with large ones. Further exchange would be possible only when the large polyelectrolyte undergoes an important modification of its solution conformation, which necessarily is time consuming.

The last point is that surface exclusion chromatography of pure polyelectrolytes by cutting the column into portions to separate the small polyelectrolytes from the large ones, as imagined from inspection of the chromatograms obtained for mobile adsorption, may constitute an impossible challenge. Therefore, selective retention on a filter soaked in a solution of polydisperse system may be employed to preferentially extract large polyelectrolytes. This information is very important if surface force measurements on a polyelectrolyte-coated sheet or sphere are intended.

Finally, these investigations demonstrate that selectivity in adsorption of polyelectrolytes adsorbing on a charged interface is obtained by a rapid exchange between adsorbed and solution macromolecules. For neutral systems like polyacrylamide in the presence of an aluminum/silicium oxide/water interface, where hydrogen bonds are responsible of adsorption, interfacial exchange between polymers of equal molecular weight was found to be very slow.[31,32] Unpublished results concerning the exchange between polymers of different molecular weight showed that the exchange rate remained slow.[33]

**Acknowledgment.** The referees are acknowledged for their pertinent remarks and their significant contributions improving the clarity of presentation of the manuscript.

## References and Notes

(1) Napper, D. H. *Polymeric Stabilization of Colloidal Dispersions;* Academic Press: New York, 1983.
(2) Hlady, V.; Lyklema, J.; Fleer, G. J. *J. Colloid Interface Sci.* **1982**, *87*, 395.
(3) Koopal, L. K. *J. Colloid Interface Sci.* **1981**, *83*, 116.
(4) Felter, R. E.; Ray, L. N. *J. Colloid Interface Sci.* **1970**, *32*, 349.
(5) Cohen Stuart, M. A.; Scheutjens, J. M. H. M.; Fleer, G. J. *J. Pol. Sci.: Pol. Phys. Ed.* **1980**, *18*, 559.
(6) Furusawa, K.; Yamashita, K.; Konno, K. *J. Colloid Interface Sci.* **1982**, *86*, 35.
(7) Elaissari, H.; Haouam, A.; Huguenard, C.; Pefferkorn, E. *J. Colloid Interface Sci.* **1992**, *149*, 68.
(8) Pefferkorn, E.; Nabzar, L.; Carroy, A. *J. Colloid Interface Sci.* **1985**, *106*, 94.
(9) Ringenbach, E.; Chauveteau, G.; Pefferkorn, E. *J. Colloid Interface Sci.* **1995**, *171*, 218.
(10) Pefferkorn, E.; Jean-Chronberg, A. C.; Chauveteau, G.; Varoqui, R. *J. Colloid Interface Sci.* **1990**, *137*, 66.
(11) Blaakmer, J.; Cohen Stuart, M. A.; Fleer, G. J. *J. Colloid Interface Sci.* **1990**, *140*, 314.
(12) Kitchener, J. A. In *The Scientific Basis of Flocculation*; Ives, K. J., Ed.; Nato Advanced Study Institutes Series, E: Applied Science-No. 27, Sithoff & Noordhoff: The Netherlands, 1978.
(13) Pefferkorn, E.; Carroy, A.; Varoqui, R. *J. Polym. Sci.: Polym. Phys. Ed.* **1985**, *23*, 1997.
(14) Pefferkorn, E.; Elaissari, A. *J. Colloid Interface Sci.* **1990**, *138*, 187.
(15) Feder, J.; Giaever, I. *J. Colloid Interface Sci.* **1980**, *78*, 144.
(16) Onoda, G. Y.; Liniger, E. G. *Phys. Rev. A* **1986**, *33*, 75.
(17) Joppien, G. R. *J. Phys. Chem.* **1978**, *82*, 2210.
(18) Cafe, M. C.; Robb, I. D. *J. Colloid Interface Sci.* **1982**, 86, 411.
(19) Huguenard, C.; Elaissari, A.; Pefferkorn, E. *Macromolecules* **1994**, *27*, 5277.
(20) Elaissari, A.; Chauveteau, G.; Huguenard, C.; Pefferkorn, E. *J. Colloid Interface Sci.* **1995**, *173*, 221.
(21) van de Ven, T. G. M. *Adv. Colloid Interface Sci.* **1994**, *48*, 121.
(22) Elaissari, A.; Pefferkorn, E. *J. Colloid Interface Sci.* **1991**, *143*, 85.
(23) Elaissari, A.; Pefferkorn, E. *J. Colloid Interface Sci.* **1991**, *141*, 522.
(24) Cantow, M. J. R. *Polymer Fractionation*; Academic Press: New York, 1967.
(25) Whatman, Technical Catalogue, No. 9037 9341, 1996).
(26) Talbot, J.; Schaaf, P. *Phys. Rev. A* **1989**, *40*, 422.
(27) Hinrichsen, E. L.; Feder, J.; Jossang, T. *J. Stat. Phys.* **1986**, *44*, 793.
(28) Varoqui, R.; Tran, Q. K.; Pefferkorn, E. *Macromolecules* **1979**, *12*, 831.
(29) Carroy, A, Thesis ULP, Strasbourg, France, 1986.
(30) Gramain, Ph.; Myard, Ph. *J. Colloid Interface Sci.* **1981**, *84*, 114.
(31) Pefferkorn, E.; Carroy, A.; Varoqui, R. *J. Polym. Sci.;Polym. Phys. Ed.* **1985**, *23*, 1997.
(32) Pefferkorn, E.; Haouam, A.; Varoqui, R. *Macromolecules* **1989**, *22*, 2677.
(33) Carroy, A. Unpublished results.

MA9605154